

Permeability of rapid prototyped artificial bone scaffold structures

Marcin Lipowiecki¹, Marketa Ryvolova^{1,2}, Akos Tottosi¹, Sumsun Naher¹ and Dermot Brabazon¹

¹ School of Mechanical and Manufacturing Engineering, Dublin City University, Glasnevin, Dublin, 9, Ireland

² Department of Chemistry, Faculty of Science, Masaryk University, Kotlářská 2, Brno, Czech Republic

Abstract.

Fluid flow through a bone scaffold structure is an important factor in its ability to build up a living tissue. Permeability is often used as a measure of a structure's ability to allow for flow of nutrients and waste products related to the growth of new tissue. These structures also need to meet conflicting mechanical strength requirements to allow for load bearing. In this work, the effect of different bone structure morphologies on permeability were examined both numerically and experimentally. Cubic and hexagonal based three dimensional scaffold structures were produced via stereolithography and 3D printing techniques. In particular, porosity percentage, pore size, and pore geometry were examined. Porosity content was varied from 30% to 70% and pore size from 0.34 mm to 3 mm. An adapted Kozeny-Carmen numerical method was applied for calculation of permeability through these structures and an experimental validation of these results was performed via a standard permeability experimental testing set-up. From the results it was determined that increased permeability was provided with the cubic rather than hexagonal structure as well as by utilizing the larger pore size and higher levels of porosity. Stereolithography was found to be the better processing technique, not only for improved micrometer scale dimensional accuracy reasons, but also due to the increase wettability found on the produced surfaces. The appropriate model constants determined in this work will allow for analysis of new alternate structure designs on the permeability of rapid prototyped synthetic bone structures.

Keywords: Permeability, porosity, artificial scaffold, bone tissue, surface tension, rapid prototyping

Introduction

Synthetic scaffold bone structures are used during surgery to aid bone repair and orthopaedic implant attachment. These structures need to meet mechanical strength and permeability requirements to allow for load bearing and osteoconductivity respectively. To increase osteoconductivity, the structure has to be designed to allow for flow of nutrients and waste products related to the growth of new tissue. Fluid flow through a bone scaffold structure is therefore an important factor in its ability to build up a living tissue. Permeability is often used as a measure of a structure's ability to allow for this. To create a successful bone implant, certain criteria must be fulfilled: 1) a biocompatible material must be used; 2) the

ideal pore size and porosity must be applied to provide required permeability and mechanical structural strength. Nowadays, there is a wide range of biocompatible materials available for tissue engineering. Ceramic-based scaffolds are also an important group of structures for skeletal implants due to their inertness and similarity of physical properties to natural bone. Scaffolds developed by foaming sol—gel derived bioactive glasses were characterised in work of Jones et al. [1]. In their work the interconnectivity of pores was tested and it was found that permeability of the scaffolds fabricated by this method was comparable to trabecular bone. Porous commercial tantalum metal grafting material (Trabecular Metal™) were previously characterised with porosity levels from 66% - 88% were tested for various parameters such as tangent elastic modulus, yield stress, strain behaviour and intrinsic permeability [2]. From this material, the intrinsic permeability and corresponding tangent elastic modulus of these structures were found to be similar to cancellous bone structures of comparable porosity. Another group of scaffold types recently reviewed are collagen or collagen-based structures. In a study presented by Al-Munajjed et al., the permeability and the porosity of hyaluronan-collagen scaffolds was tested [3]. The permeability was determined empirically and experimentally from which the relationship between increasing porosity and permeability with increasing pore size was determined. There is an increased interest in recent years in polymer based scaffolds which were recently reviewed by Cheung et al. [4]. PMMA scaffolds have been found to be suitable for manufacturing of highly porous scaffolds with controllable elastic modulus and permeability [5].

Several experimental studies have conducted to measure the permeability of real bone [5-6]. In the work of Beaudoin et al. [6] permeability values ranging between 3×10^{-9} and 16×10^{-9} m² in the direction of trabecular orientation was determined using high-viscosity silicone. These results are comparable to the values obtained in the study of Grimm and Williams where permeability for human calcaneal trabecular bone in the range $0.40 - 10.97 \times 10^{-9}$ m² were obtained using raw linseed oil [7]. Kohles et al. used water to measure permeability of cancellous bones from mature bovines [8]. The bovine bone sample produced values in the range of magnitudes (10^{-10} to 10^{-9} m²) similar to previous investigations. It is important to have similar values of pore size and permeability in artificial bone structures compared to real bone. Usually water solutions are used for this type of permeability testing.

A lot of this previous research work has focused on the biocompatibility and mechanical strength of artificial bone structures. There remains a corresponding lack of work on the investigation of the permeability of these structures. In this work two different structures (cubic and hexagonal), previously investigated for mechanical strength capability in bone scaffold production, were compared for permeability [9]. These structure types provide a high stiffness combined with a high porosity and pore size. The structures were produced by rapid prototyping methods allowing pre-definition of the pore size, porosity, and external geometry. The goal of this work was to measure the permeability coefficients of these new structures and to develop a method to determine the appropriateness of the various new designs in terms of permeability.

2. Experimental

The 3D cubic and hexagonal samples (as shown in Fig. 1) were manufactured using a Z310 Z-Corp 3D printer and a common 3D printing powder material ZP 113 (plaster — calcium sulphate) and binder ZB-58 (epoxy) were used. To reinforce the specimens, infiltration using the epoxy ZMax resin was performed. The models are designed using computer aided design software SolidEdge V100, PTC and saved as stereolithography files. To evaluate the structures purely from a permeability point of view, no biocompatibility is needed and therefore these standard plaster-based powder and epoxy resin materials were used. Models were also produced in polyurethane via the micro-stereolithography technique, which allows for components of smaller dimension and higher accuracy, supplied by Hordler Rapid Engineering GmbH, Germany.

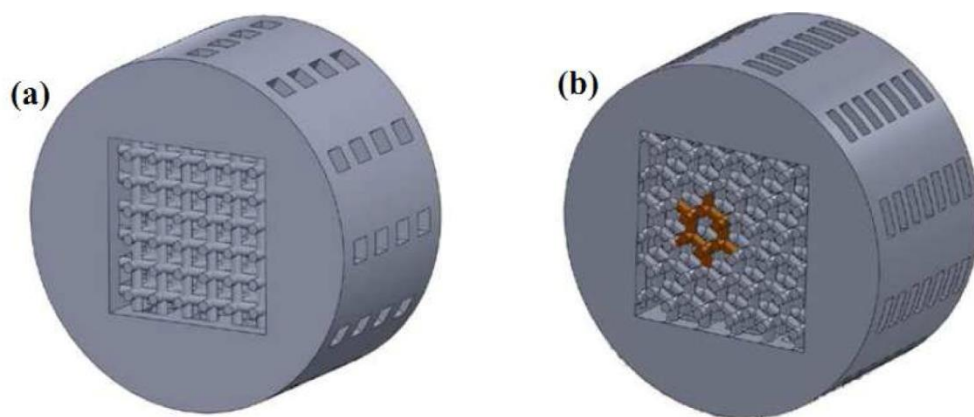


Fig. 1: CAD images of the investigated (a) cubic and (b) hexagonal structures with supporting collar and as fabricated for permeability testing.

The cubic structure was omni-directional, and therefore the test was only conducted along one axis. Testing for the hexagonal structure was performed along the direction with the largest pore area presenting to the fluid flow. The pore size was defined as the length of the strut for one edge of the cube structure and as the diameter of the circle which could be inscribed within the presenting hexagonal area. Hexagonal structures were fabricated with a second defining length, which was the height between layers. The external boundary of a larger set of these structures was a 15x15x15 mm cube with an internal pore size and porosity level ranging 0.34 to 3 mm and 30% to 70% respectively. Another smaller set of structures within an external boundary of 3x3x3 mm contained a pore size ranging from 0.6 to 0.34 mm, also designed with a porosity ranging from 30% to 70%. Each of three conditions was fabricated and tested three times to test for repeatability.

Specimens fabricated via the 3D printing method were cleaned using compressed air and then infiltrated using the epoxy resin. The infiltration process was implemented by dipping each specimen into the resin mixture and then exposed to a reduced atmospheric pressure (0.2 Bar) for 3 minutes to improve infiltration. This process was repeated three times to provide for maximal infiltration. The infiltrated specimens were left to dry over the night. Subsequently

the horizontal pores were blocked using tape and by the sample receptacle of the permeability setup (see Fig. 2) during testing to prevent liquid leakage when exposed to the liquid flow. Water-glycerol solution (Sigma Aldrich) was employed to simulate a level of viscosity within the range typically found for blood viscosity, which is in the range from 3 to 6 times higher than water depending on the hematocrit, blood flow rate, and blood constituents such as proteins, nutrients, hormones and excretory products [10].

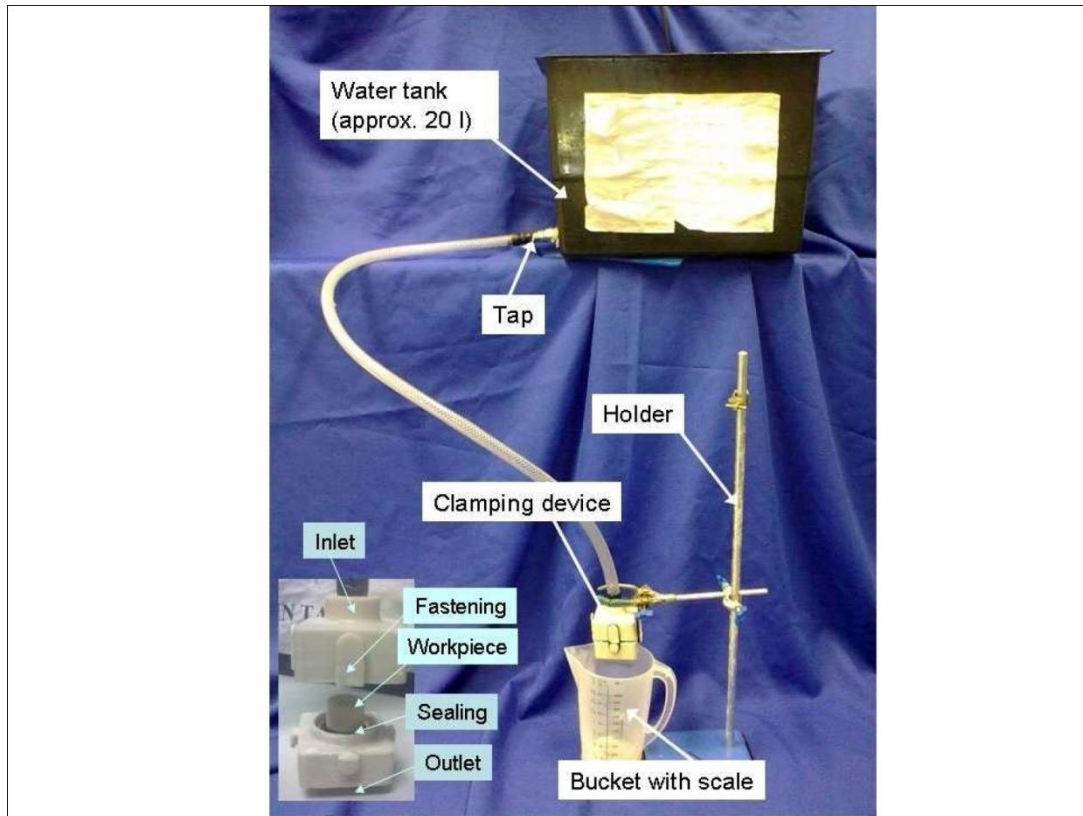


Fig. 2: Schematic of the setup for synthetic bone scaffold permeability measurement with inset showing sample receptacle.

Blood typically varies from 3 mPas to 6 mPas while blood without cells is typically in the range from 1 to 1.3 mPas. In this work the viscosity of the glycerol solution was recorded at 3.6 mPas using a rotational viscometer (Rheology International Instrument, ASTM Spindle Type2).

For permeability measurement, the principle of the measurement was to let water flow through different samples, and measure the fluid volume and time. A liquid tank (500x300x400 mm) was used and the measured volume was 500 ml. The large tank provided constant hydrostatic pressure and as the height difference, A_h , was set at 800 mm. The hydrostatic pressure was calculated as follows: $\rho_{in} = \rho_g \Delta h g = 8066 \text{ Pa}$ for glycerol- water solution, where $\rho_{\text{glycerol/water}} = 1027.78 \text{ kg/m}^3$.

3. Results and discussion

Figure 3 shows experimental results determined from the cubic and hexagonal structures for different pore sizes and percentages of porosities. The Kozeny-Carman formula, first proposed by Kozeny and later refined by Carman, is commonly used to predict permeability and has many forms. The theory is based on the classical Navier-Stokes fluid mechanics, like fluid flowing in capillaries [26]. The form used in this work to determine the permeability factor, K , in units of m^2 was as follows:

$$K = C \times \frac{g}{\mu_w \rho_w} \times \frac{e^3}{S^2 D_r^2 (1+e)}$$

C = constant

μ_w = dynamic viscosity of water, Pa s

ρ_w = density of fluid, kg/m^3

e = porosity

$$S = \frac{\text{surface area}}{\text{mass of solid}} \left[\frac{m^2}{kg} \right]$$

$$D_r = \frac{\text{density of solid}}{\text{density of fluid}}$$

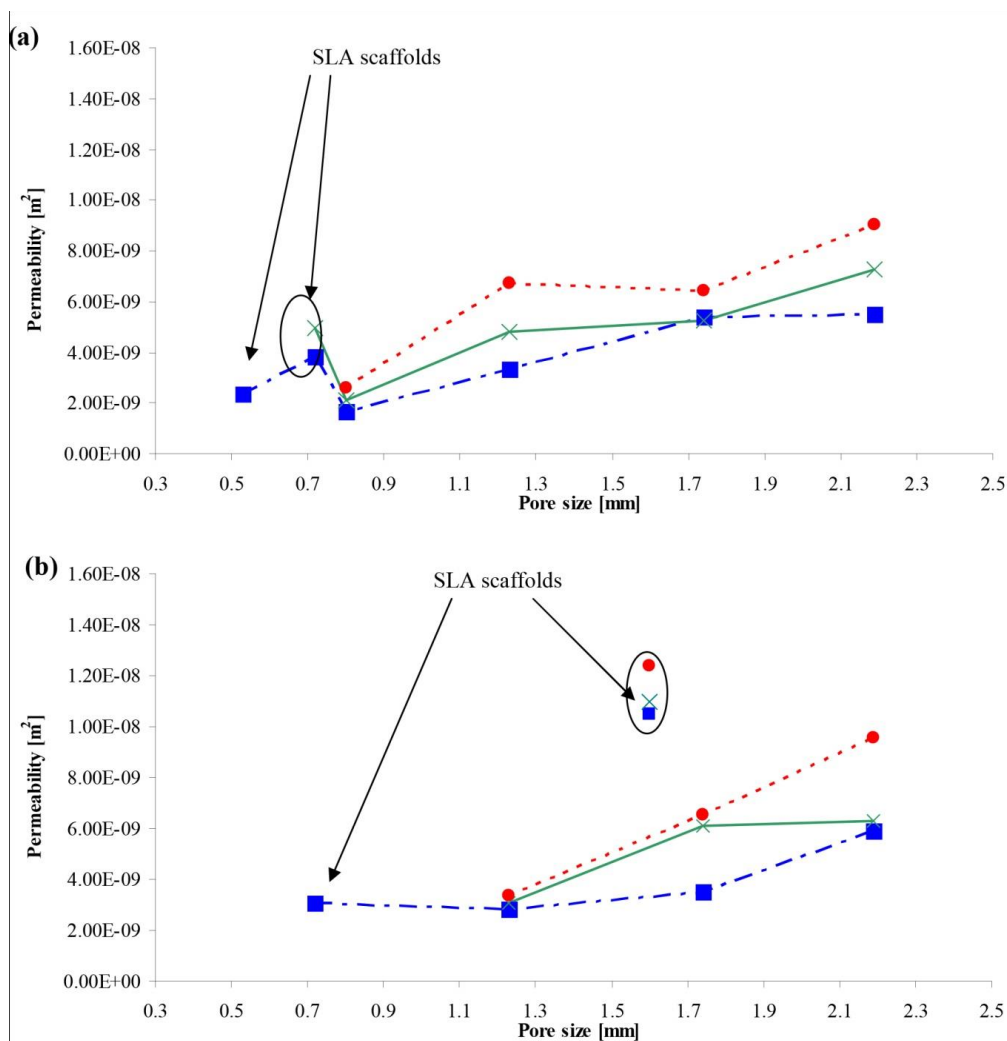
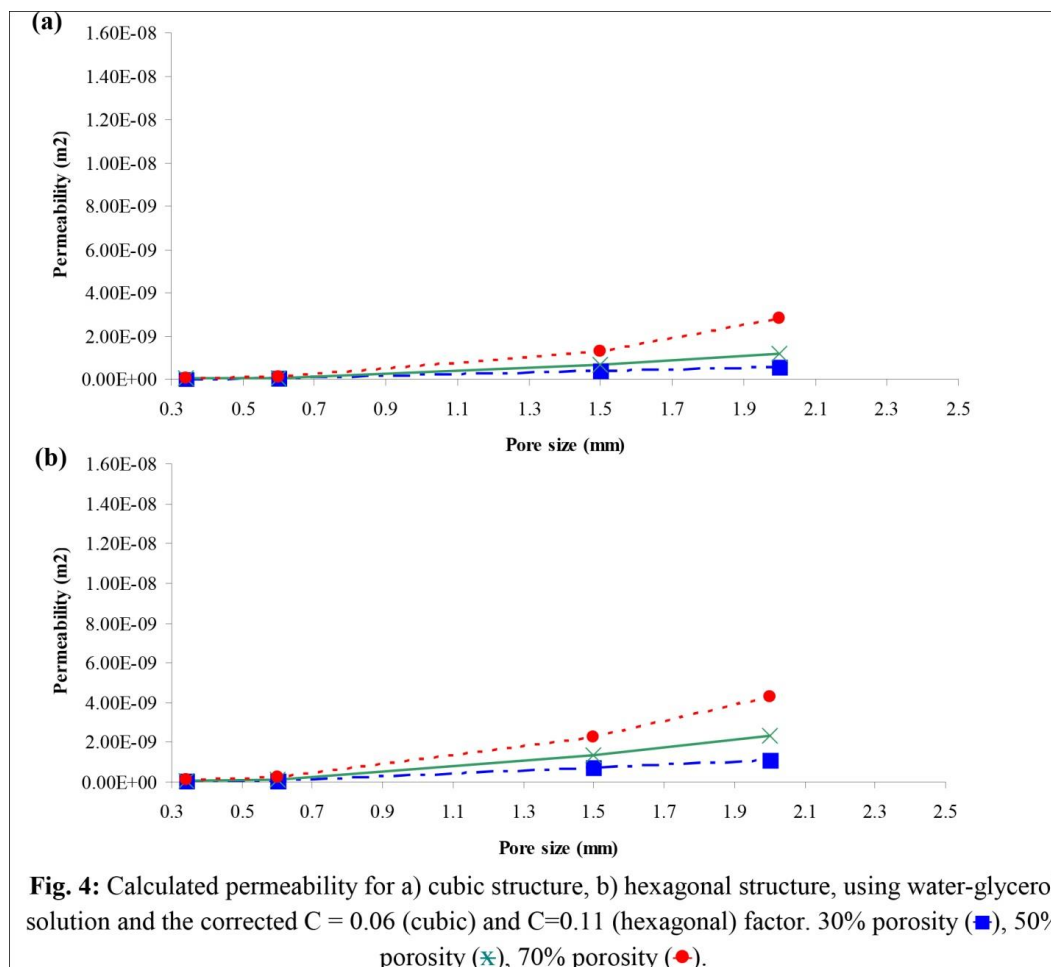


Fig 3: Measured permeability obtained for (a) cubic and (b) hexagonal structures using glycerol-water solution through structures with 30% porosity (■), 50% porosity (x), 70% porosity (●) and various pore sizes.

The constant C is used for describing the shape of the particles. As a first approximation, a value of 0.2 was used for C , selected from previous data based on the experimental work of Chapuis [11] . This constant was re-calculated based on the findings of the experimental work presented Fig. 3. The "specific surface" is the one of the most critical parameters. The whole solid surface of the structure, measured directly from the CAD models was used to calculate the specific surface. The newly determined corrected C factors, $C = 0.06$ for the cubic structures and $C = 0.11$ for the hexagonal structures, were used in the Kozeny-Carman model to determine the permeabilities of these structures. Figure 4 shows the results calculated from the adapted Kozeny-Camen model.



Conclusion

From the results it clear that the experimental method used in this work are capable of producing good comparison of permeability through different bone scaffold structures. The permeability values determined in this study correspond well with the range of results from other researches. In particular the cubic structure showed permeability values ranging from 1×10^{-8} m² to 2×10^{-9} m² for these structures. The cubic structure, large pores sizes and higher porosity contents were found to provide increased permeability. For the real bone

structures, the pore size typically ranges from 100 to 500 pm and in this range, the calculated permeabilities fitted well to the measured values. The permeability depends on the surface area of the whole structure, on the material surface, the internal structure, and on the applied flow fluid. The greatest influence was caused by the pore size with less effect evident from different porosity levels at the lower pore sizes. The ideal permeability may be determined as that which is currently found in natural bone materials or higher permeability might be preferable for new scaffolds. This work presents a method whereby the desired permeability level can be achieved by design and tested experimentally and numerically.

References

- [1] J.R. Jones, G. Poologasundarampillai, R.C. Atwood, D. Bernard and P.D. Lee, *Biomaterials* 2007, 28, 1404-1413.
- [2] D.A., Shimko, V.F. Shimko, E.A. Sander, K.F. Dickson, E.A. Nauman, *Journal of Biomedical Materials Research Part B-Applied Biomaterials* 2005, 73B, 315-324.
- [3] A.A. Al-Munajjed, M. Hien, R. Kujat, J.P. Gleeson, and J. Hammer, *Journal of Materials Science: Materials in Medicine* 2008, 19, 2859-2864.
- [4] H.Y. Cheung, K.T. Lau, T.P. Lu and D. Hui, *Composites Part B-Engineering* 2007, 38, 291.
- [5] D.A. Shimko, E.A. Nauman, *Journal of Biomedical Materials Research Part B-Applied Biomaterials* 2007, 80B, 360-369.
- [6] A.J. Beaudoin, W.M. Mihalko, W.R. Krause, *Journal of Biomechanics* 1991, 24, 127.
- [7] M.J. Grimm and J.L. Williams, *Journal of Biomechanics* 1997, 30, 743-745.
- [8] S.S. Kohles, J.B. Roberts, M.L. Upton, C.G. Wilson, L.J. Bonassar, and A.L. Schlichting, *Journal of Biomechanics* 2001, 34, 1197-1202.
- [9] M. Lipowiecki and D. Brabazon, *Advanced Materials Research*, Vol. 83-86, 2010, pp. 914-922.
- [10] R.S. Rosenson, A. McCormick, and E.F. Uretz, *Clinical Chemistry* 1996, 42, 1189-1195.
- [11] R.P. Chapuis and M. Aubertin, *EPM-RT-2003 03*, Ecole Polytechnique, Montreal, Que 2003.